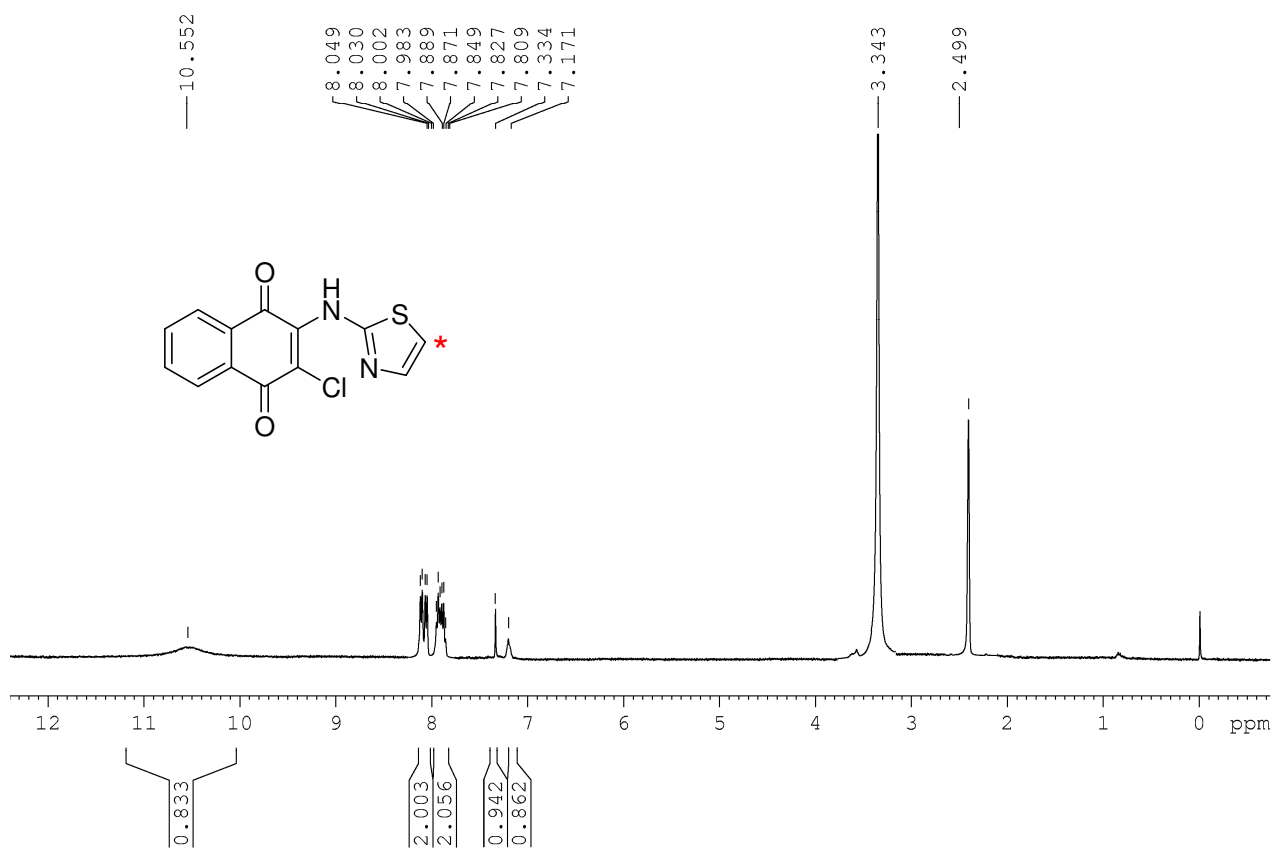


## Highly selective colorimetric sensing of Hg(II) ion in aqueous medium and solid state via formation novel M-C bond

C.Parthiban, R.Manivannan and Kuppanagounder P. Elango\*

### Table of Content

- Fig. S1.**  $^1\text{H}$  NMR spectrum of R1
- Fig. S2.**  $^{13}\text{C}$  NMR spectrum of R1
- Fig. S3.** LCMS spectrum of R1
- Fig. S4.** Colour change of receptor in aqueous solution (DMF:H<sub>2</sub>O; 1:9 v/v) in presence of various metal ions.
- Fig. S5.** UV-Vis spectral changes of the receptor upon the addition of the different cations.
- Fig. S6.** Fluorescence changes of R1 ( $6.5 \times 10^{-4}$  M) upon addition of Hg(II) ( $0-2.5 \times 10^{-3}$  M) in DMF: H<sub>2</sub>O (1:9 v/v).
- Fig. S7.** Benesi-Hildebrand plot of the receptor with Hg(II).
- Fig. S8.** Job's plot of R1( $2.5 \times 10^{-4}$  M) upon addition of Hg(II).
- Fig. S9.** Detection limits plot of the receptor.
- Table S1.** Crystal data and structure refinement for Hg(II) complex.
- Fig. S10.** Packing diagram of Hg(II) complex.
- Fig. S11.** Optimized geometry of the receptor R1.
- Fig. S12.** Mullikan Chagres of the receptor R1.
- Fig. S13.** Color changes of the test papers for detecting Hg(II) in aqueous solution with different concentrations.



**Fig. S2.**  $^1\text{H}$  NMR spectrum of R1

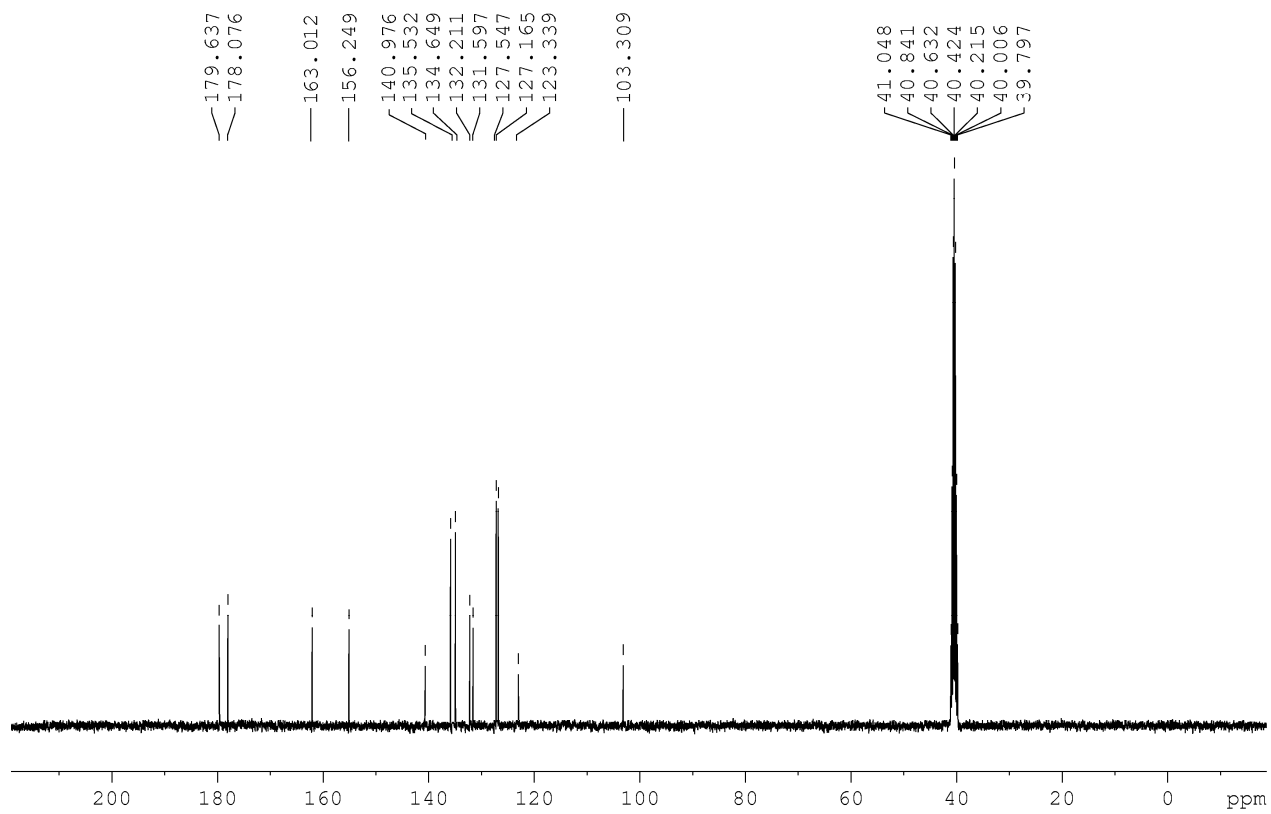


**Fig. S2.**  $^{13}\text{C}$  NMR spectrum of R1

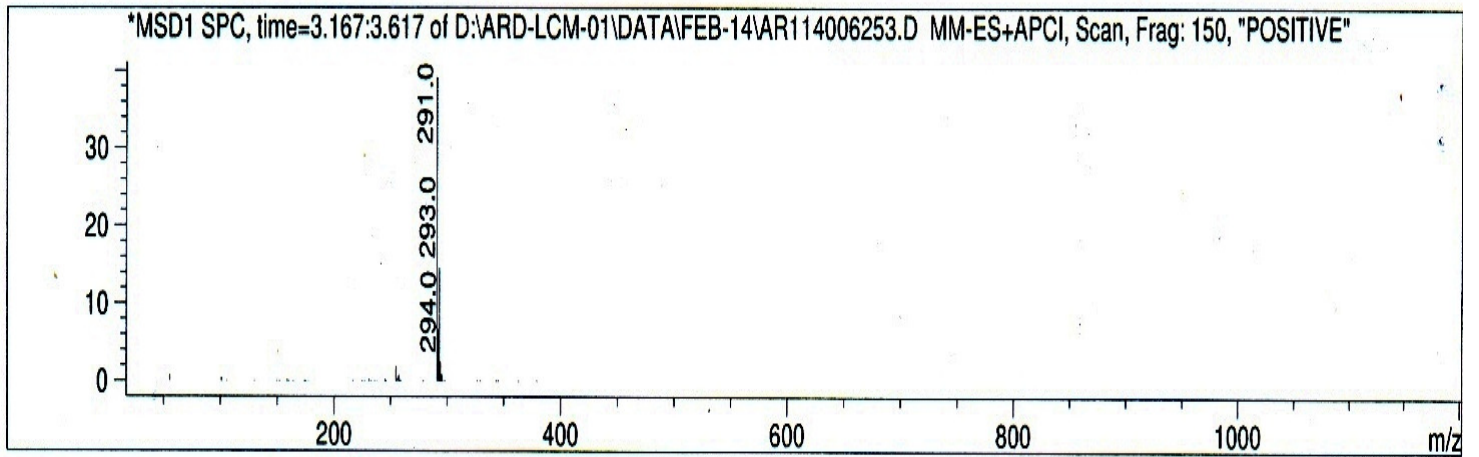


**Fig. S3.** LCMS spectrum of R1



R Hg(II) Na(I) K(I) Mg(II) Ca(II) Ba(II) Pb(II) Fe(III) Co(II) Ni(II) Cu(II) Zn(II) Cd(II)

**Fig. S4.** Colour change of receptor in aqueous solution (DMF:H<sub>2</sub>O; 1:9 v/v) in presence of various metal ions.

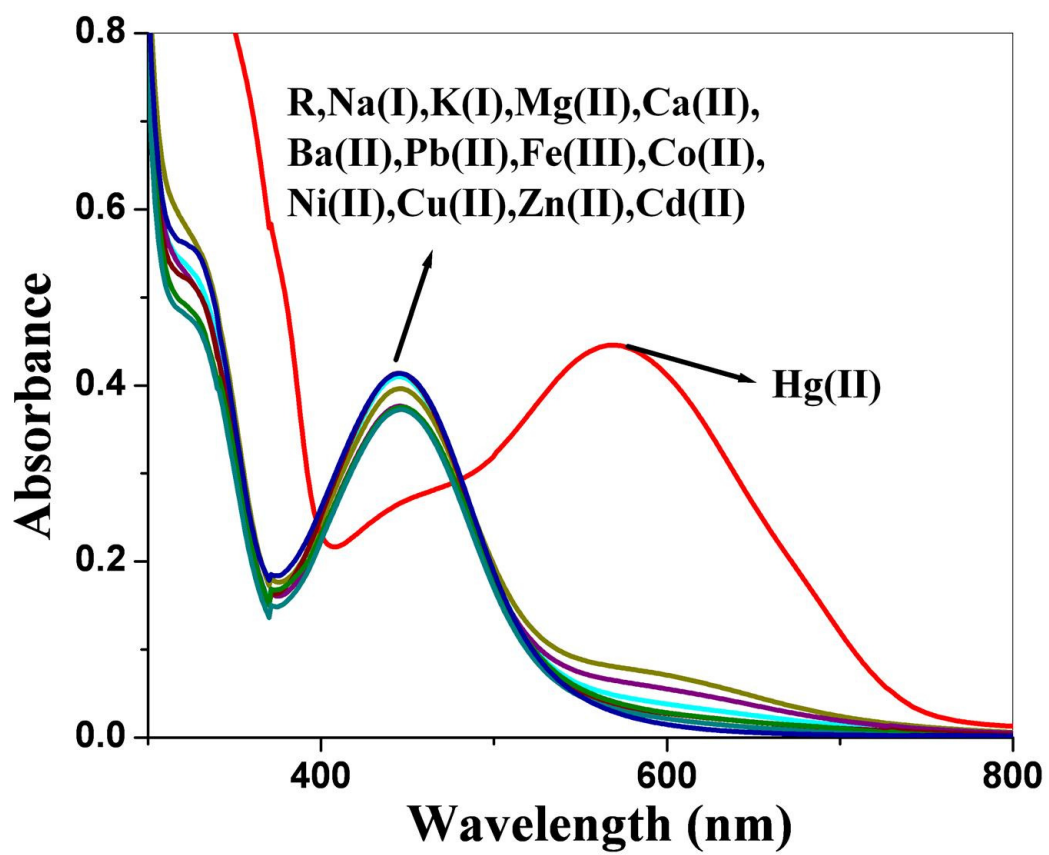


**Fig. S5.** UV-Vis spectral changes of the receptor upon the addition of the different cations.

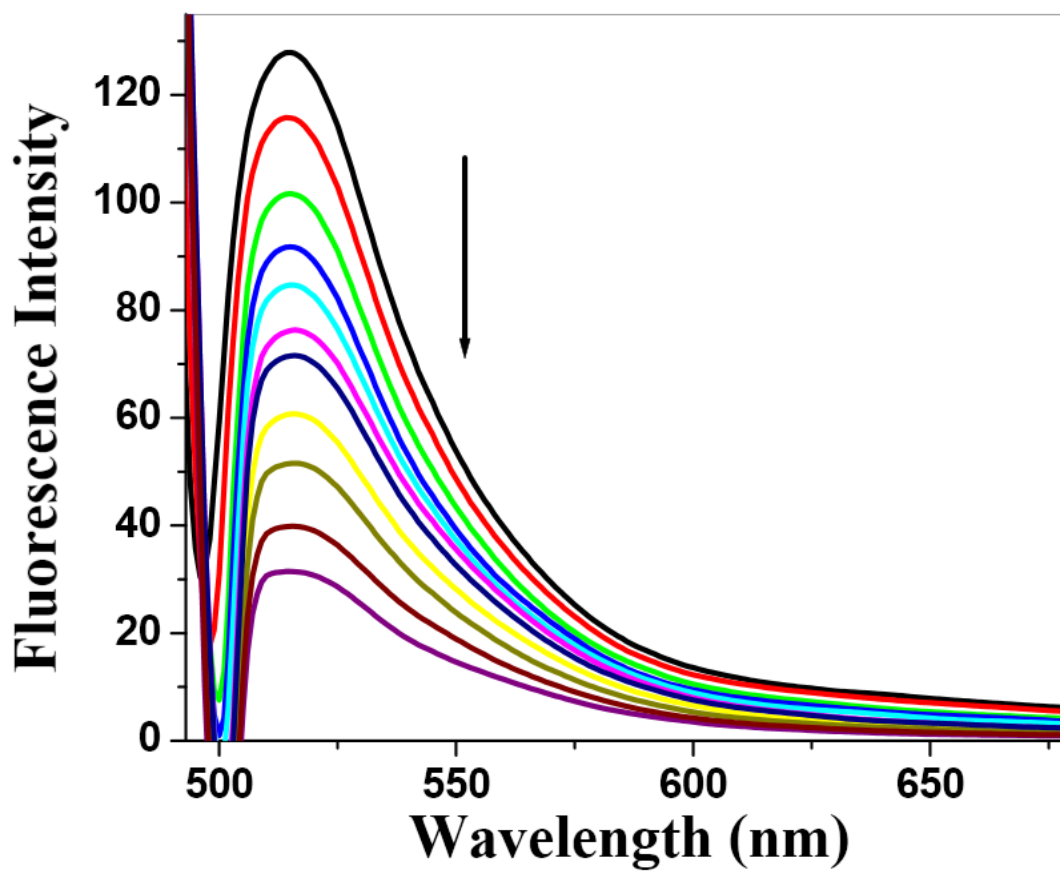


**Fig. S6.** Fluorescence changes of R1( $6.5 \times 10^{-4}$  M) upon addition of Hg(II) (0- $2.5 \times 10^{-3}$  M) in DMF: H<sub>2</sub>O (1:9 v/v).

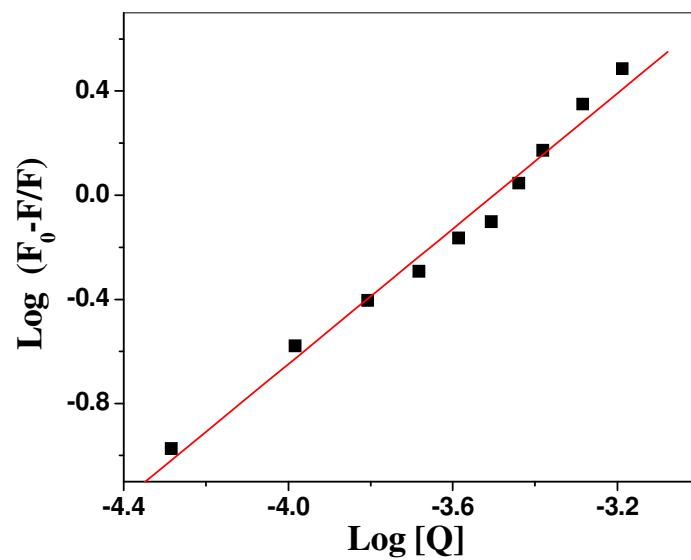


**Fig. S7.** Benesi-Hildebrand plot of the R1 with Hg(II).



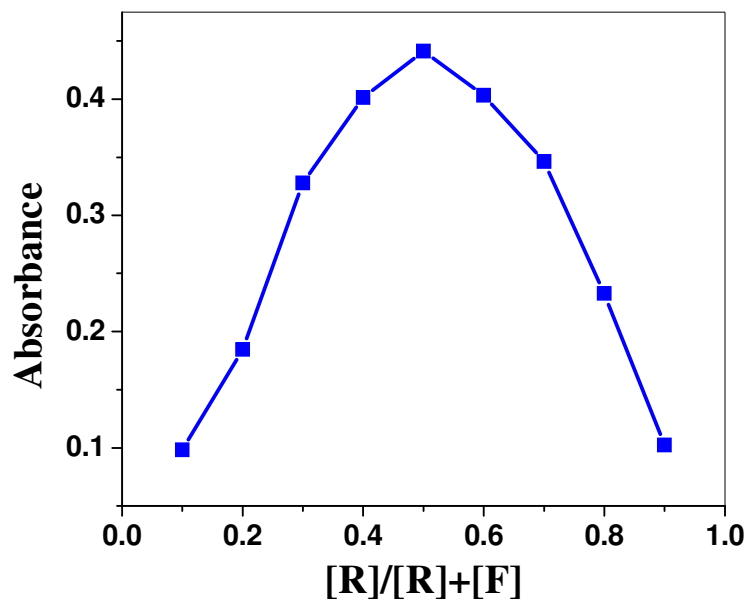


**Fig. S8.** Job's plot of R1 ( $2.5 \times 10^{-4}$  M) upon addition of Hg(II).

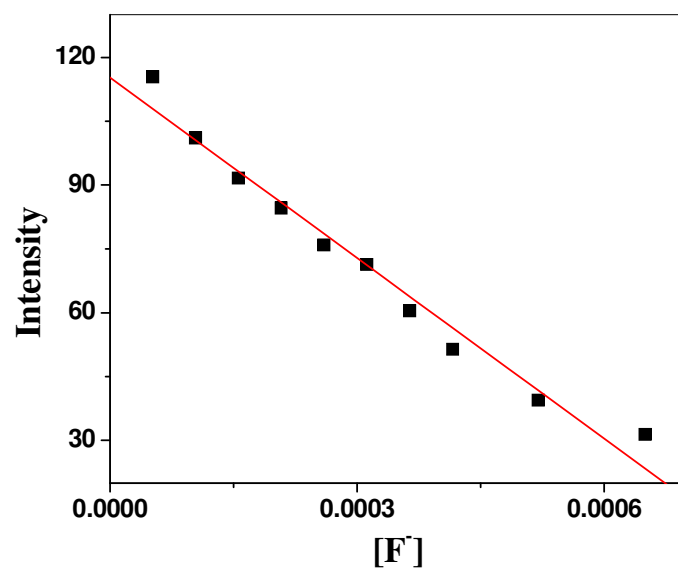


**Fig. S9.** Detection limits plot of the receptor.

---

**Table S1.** Crystal data and structure refinement for the Hg(II) complex.

---

Empirical formula	C <sub>16</sub> H <sub>13</sub> Cl <sub>2</sub> HgN <sub>3</sub> O <sub>3</sub> S
Formula weight	598.84
Temperature	293(2) K
Wavelength	0.71073 Å
Crystal system, space group	Monoclinic, P21/c
Unit cell dimensions	a = 12.9121(5) Å    alpha = 90 deg. b = 7.7803(3) Å    beta = 94.4640(10) deg. c = 18.6223(8) Å    gamma = 90 deg.
Volume	1865.12(13) Å <sup>3</sup>
Z, Calculated density	4, 2.133 Mg/m <sup>3</sup>
Absorption coefficient	8.672 mm <sup>-1</sup>
Crystal size	0.35 x 0.30 x 0.25 mm
Theta range for data collection	2.19 to 26.00 deg.
Limiting indices	-15<=h<=15, -9<=k<=9, -22<=l<=22
Reflections collected / unique	26561 / 3661 [R(int) = 0.0471]
Completeness to theta = 26.00	100.0 %
Absorption correction	Semi-empirical from equivalents
Max. and min. transmission	0.2294 and 0.1503
Refinement method	Full-matrix least-squares on F <sup>2</sup>
Data / restraints / parameters	3661 / 1 / 239
Goodness-of-fit on F <sup>2</sup>	1.187
Final R indices [I>2sigma(I)]	R1 = 0.0336, wR2 = 0.0899
R indices (all data)	R1 = 0.0500, wR2 = 0.0970
Largest diff. peak and hole	0.765 and -0.942 e.Å <sup>-3</sup>

---

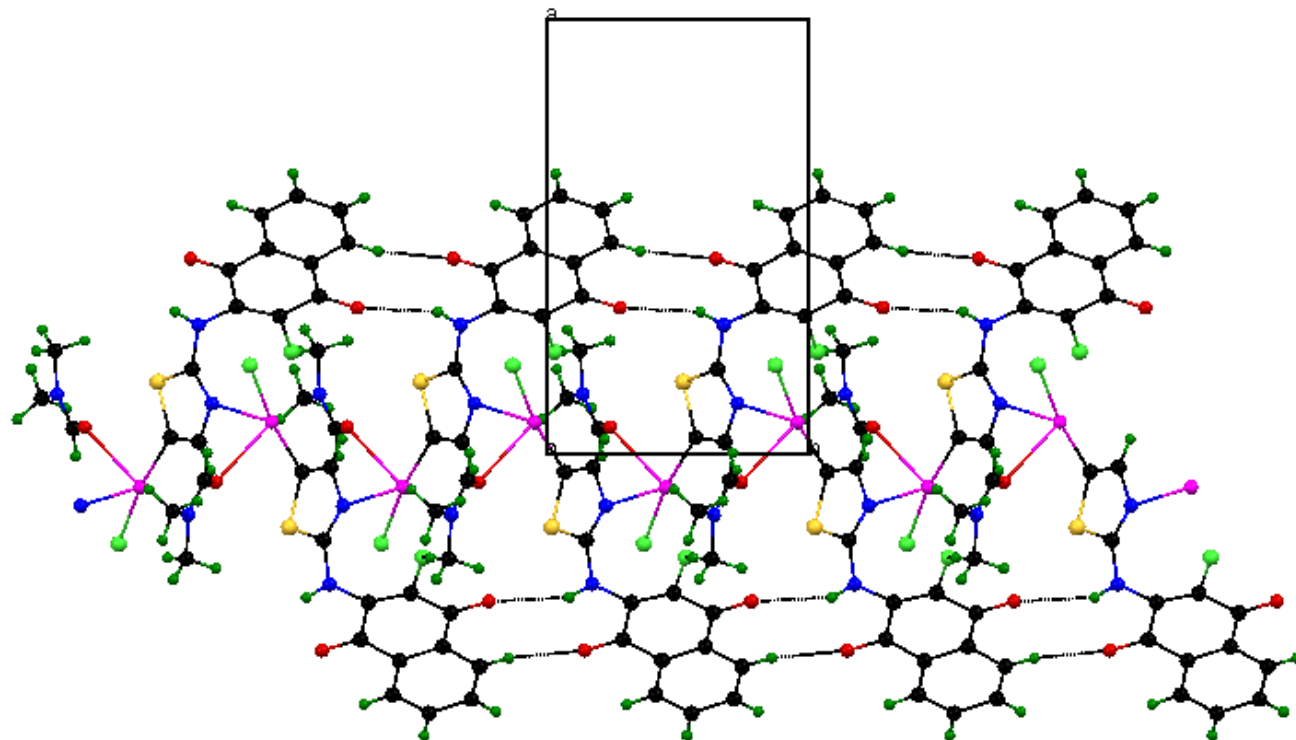


**Fig. S10.** Packing diagram of the Hg(II) complex.

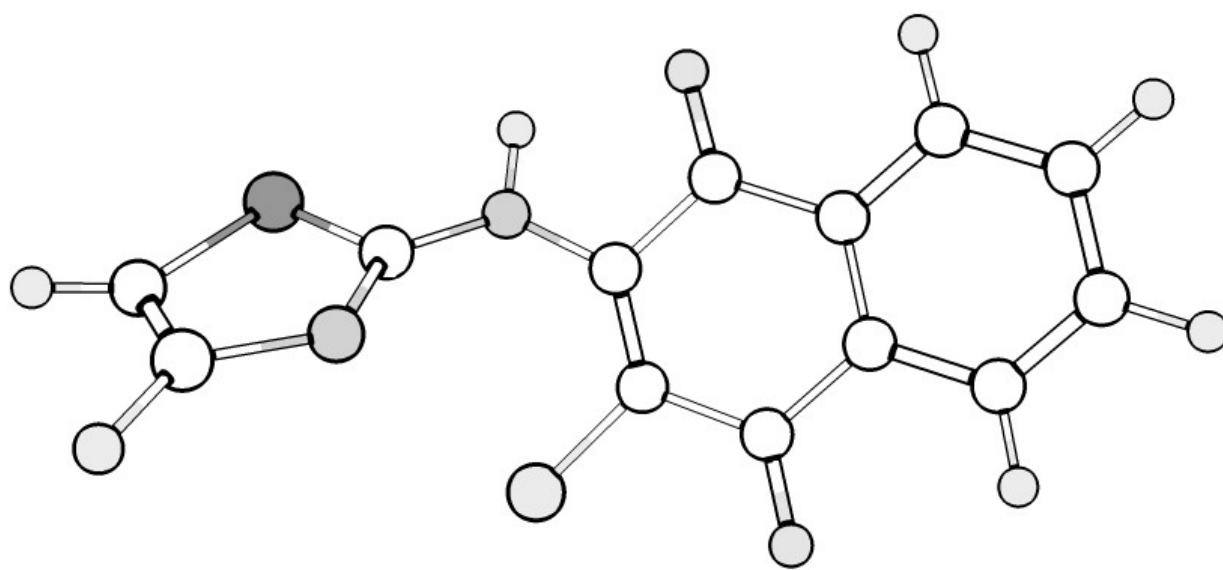


**Fig. S11.** Optimized geometry of the receptor R1.

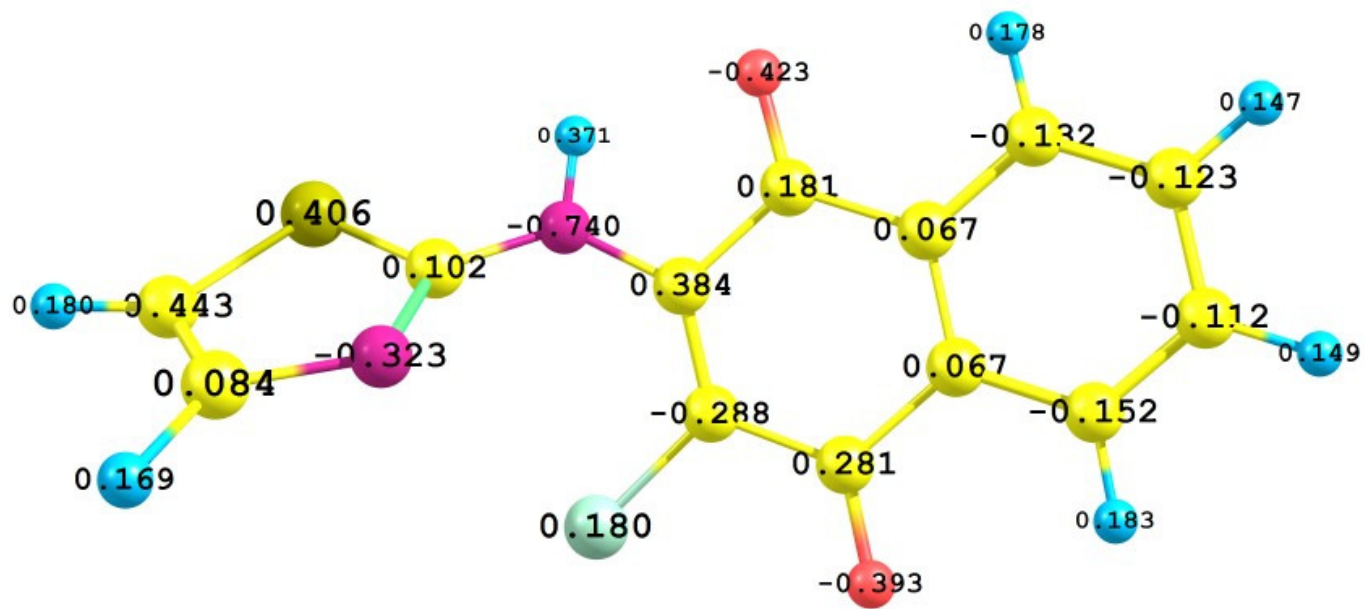


**Fig. S12.** Mulliken Charges of the receptor R1.

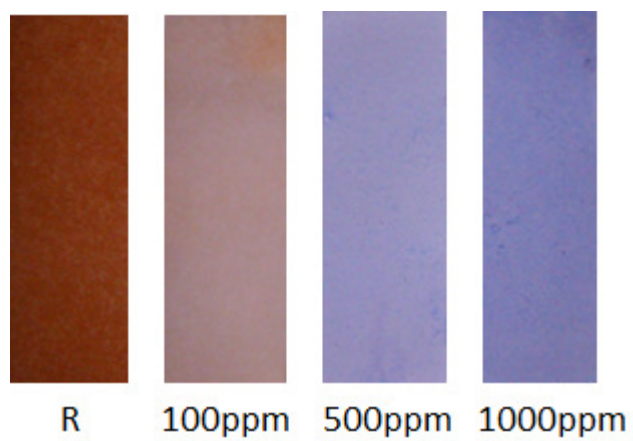


**Fig. S13.** Color changes of the test papers for detecting Hg(II) in aqueous solution with different concentrations.